Available online at www.sciencedirect.com
SciVerse ScienceDirect
Energy Procedia 33 (2013) 214 – 222
Energy Procedia

PV Asia Pacific Conference 2012

Effect of Annealing on the Properties of $Zn_xCd_{1-x}S$ Thin Film Growth by RF Magnetron Co-sputtering

M.S. Hossain[a], M.A. Islam[b], M.M. Aliyu[a], P. Chelvanathan[b], T. Razykov[b], K. Sopian[b], N. Amin[a,b,c,*]

[a]*Department of Electrical, Electronic and System Engineering, Faculty of Engineering and Built Environment, The National University of Malaysia, 43600 Bangi, Selangor, Malaysia*
[b]*Solar Energy Research Institute, The National University of Malaysia, 43600 Bangi, Selangor, Malaysia*
[c]*Center of Excellence for Research in Engineering Materials (CEREM), College of Engineering, King Saud University, Riyadh 11421, Saudi Arabia*

Abstract

$Zn_xCd_{1-x}S$ thin films at low zinc content have been deposited on bare soda lime glass substrates using RF magnetron co-sputtering of CdS and ZnS for the first time to investigate annealing effect on the structural and optical properties of the thin films. The as-deposited films were annealed in O_2/N_2 ambient at annealing temperature ranging 200-500 °C. The composition of the films was controlled by varying RF power of CdS and ZnS in such a ratio so that zinc content in the thin films was low. The composition, structural, optical and surface morphological properties of the films was investigated using EDX, XRD, UV-Vis spectrophotometer and FESEM. The annealed films were observed hexagonal wurtzite structure with strong preferential orientation along (002) diffraction peak. Crystallinity of the films increased with increasing annealing temperature below 400°C whereas beyond 400°C new peaks were observed along with decreasing trend of (002) diffraction peak. Optical absorption and transmission spectra were recorded within the range 300-900 nm. With increasing annealing temperature, the band gap of the annealed films once decreased and then abruptly increased at around 400°C. The decreased bandgap may have been due to possible increase in the crystalline nature of the material. From SEM, it was observed that the thin films were formed by different clusters of grains which later changed to isolated grains as the annealing temperature increased. This work confirms that annealing temperature has overbearing influence on the $Zn_xCd_{1-x}S$ thin film properties deposited by RF magnetron co-sputtering.

Selection and peer-review under responsibility of Solar Energy Research Institute of Singapore (SERIS) – National University of Singapore (NUS). The PV Asia Pacific Conference 2012 was jointly organised by SERIS and the Asian Photovoltaic Industry Association (APVIA)

Keywords: $Zn_xCd_{1-x}S$; co-sputtering; annealing; RF power; grains

* Corresponding author. Tel.: +603-8921-6325; fax: +603-8921-6146.
E-mail address: nowshad@eng.ukm.my

Selection and peer-review under responsibility of Solar Energy Research Institute of Singapore (SERIS) – National University of Singapore (NUS). The PV Asia Pacific Conference 2012 was jointly organised by SERIS and the Asian Photovoltaic Industry Association (APVIA)
doi:10.1016/j.egypro.2013.05.060

1. Introduction

II-VI compound semiconductors are of current interest of the research communities because of their wider use in the fabrication of solar cells and other opto-electronic devices, with much attention shown on cadmium sulphide (CdS) for efficient use from the simulation and fabrication of solar cells [1-4].For commercial CdS/CdTe solar cells, CdS is the typical window layer. However, CdS window layer absorbs the blue region of the solar spectrum as its bandgap is as low as 2.41 eV, which affects to decrease in short circuit current of solar cells [5]. To overcome these problems in CdS/CdTe solar cells, reducing the thickness of CdS layer to less than 100 nm is routinely done. Below 100 nm, there is a general degradation [6] in the cell performance owing to considerable decrease in shunt resistance and excessive pinhole formation across the heterojunction, which can adversely affect the device open-circuit voltage (V_{oc}) and fill factor (*FF*). Moreover, in CdS/CdTe interface the electron affinity, lattice constant and thermal mismatches result in the formation of high density of interface states which reduce the V_{oc} and accordingly the conversion efficiency of the cell [7]. For the higher performance of solar cell, substituting an alternative window layer with a higher bandgap than CdS is a promising approach. In recent years, $Zn_xCd_{1-x}S$ alloy compounds have attracted technological interest because the bandgap can be tuned in wide range and the lattice parameters can be varied [8]. The ternary $Zn_xCd_{1-x}S$ films with higher energy band gap than CdS are candidates for window layers in thin film solar cells. In heterojunction solar cells, the use of $Zn_xCd_{1-x}S$ instead of CdS can lead to an increase in photocurrent by providing a match in the electron affinities of the window and absorber material [9, 10]. $Zn_xCd_{1-x}S$ are known to have properties in between those of CdS and ZnS. In CdS/CdTe solar cells, the replacement of CdS with the higher band gap ternary $Zn_xCd_{1-x}S$ film can lead to a decrease in window absorption losses and has resulted in an increase in the short circuit current [11, 12]. It also produces higher conversion efficiency [11]. The optimisation of parameters of existing solar cells and fabrication of new designed solar cells and new optoelectronic devices repeatedly demand preparing $Zn_xCd_{1-x}S$ window layer with a controllable distribution of Zn content. Keeping these aspects in view, much attention is being given in developing high quality $Zn_xCd_{1-x}S$ thin films for comprehensive optical and structural studies and their various applications. However, some problems exist in heterojunction solar cells with the use of $Zn_xCd_{1-x}S$ thin film as a window layer due to the change in the Zn concentration within the compound changing the lattice parameters linearly. Moreover, electrical resistivity increases from 1 Ω cm at x=0.0 to 10^{12} Ω cm at x=1.0 [13]. Therefore, this work focused on the deposition and characterisation of $Zn_xCd_{1-x}S$ thin film with low Zn content (0.23%).

$Zn_xCd_{1-x}S$ thin films have been deposited in a variety of ways: vacuum evaporation [14], spray pyrolysis [15], chemical bath deposition (CBD) [16]. There have been many reports on the fabrication of $Zn_xCd_{1-x}S$ thin films with variable compositions using the CBD technique, however, a few reports are available on the fabrication of $Zn_xCd_{1-x}S$ thin film with low zinc concentration or on the effect of annealing on the structural, morphological and optical properties of the films. Moreover, there is no report on the deposition of $Zn_xCd_{1-x}S$ thin films with variable or fixed compositions prepared by RF magnetron sputtering, despite being one of the simplest methods used for the deposition of II-VI thin films. In recent literature [17], RF magnetron sputtering was reported to form TaSiN thin films by varying RF power of TaSi and $TaSi_{2.7}$ targets in an Ar/N_2 atmosphere. Keeping these aspects in view, an effort was made for the first time to prepare $Zn_xCd_{1-x}S$ thin films at low Zn content (0.23%) by RF magnetron co-sputtering of CdS and ZnS and the annealing effect on the structural, morphological and optical properties of the as-deposited films are reported and discussed.

The main focus of this study is to prepare $Zn_xCd_{1-x}S$ thin films at low zinc content as well as to improve the quality of the films by controlled annealing treatment that can be implemented in thin film CdTe solar cells specifically as a window layer.

2. Experimental

Bare soda lime glasses were cleaned in an ultra-sonic bath degreased by ethanol-acetone-ethanol and de-ionised water respectively. The time taken for each step was about 5 minutes. Degreased glasses were cleaned by dry nitrogen (N_2) gas. CdS and ZnS targets (99.999% purity) were then co-sputtered on these cleaned bare glasses by non-reactive RF magnetron sputtering in an argon gas ambient. The Kurt J. Lesker 4-gun model sputtering machine was used for sputtering of all the samples. Before starting deposition, the sputtering chamber was flushed by evacuation and purged with pure nitrogen gas for 3 times. Likewise, the targets (CdS and ZnS) was covered by the shutter and pre-sputtered for between 10-15 minutes in order to remove any oxide on the target surfaces. The RF power of CdS and ZnS was varied in such a ratio so that $Zn_xCd_{1-x}S$ was deposited in the desired composition (x=0.23). The thickness of deposited $Zn_xCd_{1-x}S$ thin films was found to be 260 nm which was confirmed from SEM cross sectional images as well as referencing the thickness monitor during deposition. Investigations showed that thickness depends on the operating pressure during sputtering besides RF power. Post deposition annealing was performed in the temperature range 200-500 °C in nitrogen/oxygen gas environment for 15 minutes with a vacuum pressure of 40 mTorr. After annealing processes had been performed, the samples were still left in the annealing chamber until they were naturally cooled down to room temperature. Table 1 shows the process parameters for deposition and annealing of $Zn_xCd_{1-x}S$ thin films prepared by RF magnetron co-sputtering.

Table 1. Process parameters for deposition and annealing of $Zn_xCd_{1-x}S$ thin films deposited on bare soda lime glasses

Sample no.	Deposition temperature (^{0}C)	Base pressure (Torr)	Operating Pressure (Torr)	Argon gas flow (sccm)	Annealing temperature (°C)
1	100	2.2×10^{-5}	1.6×10^{-2}	17	As-deposited
2	100	2.2×10^{-5}	1.6×10^{-2}	17	200
3	100	2.2×10^{-5}	1.6×10^{-2}	17	300
4	100	2.2×10^{-5}	1.6×10^{-2}	17	400
5	100	2.2×10^{-5}	1.6×10^{-2}	17	500

3. Results and discussions

The composition of $Zn_xCd_{1-x}S$ thin films was confirmed by EDX analysis. RF power of CdS and ZnS were varied in arbitrary basis during co-sputtering to get the desired composition (low value of 'x') of the films. RF power of ZnS was kept to very low value in comparison to RF power of CdS as the deposition rate of ZnS is very high than that of CdS in a constant time. EDX patterns of $Zn_xCd_{1-x}S$ thin films deposited with the parameters shown in Table 1 for different values of 'x' are shown in Fig. 1.

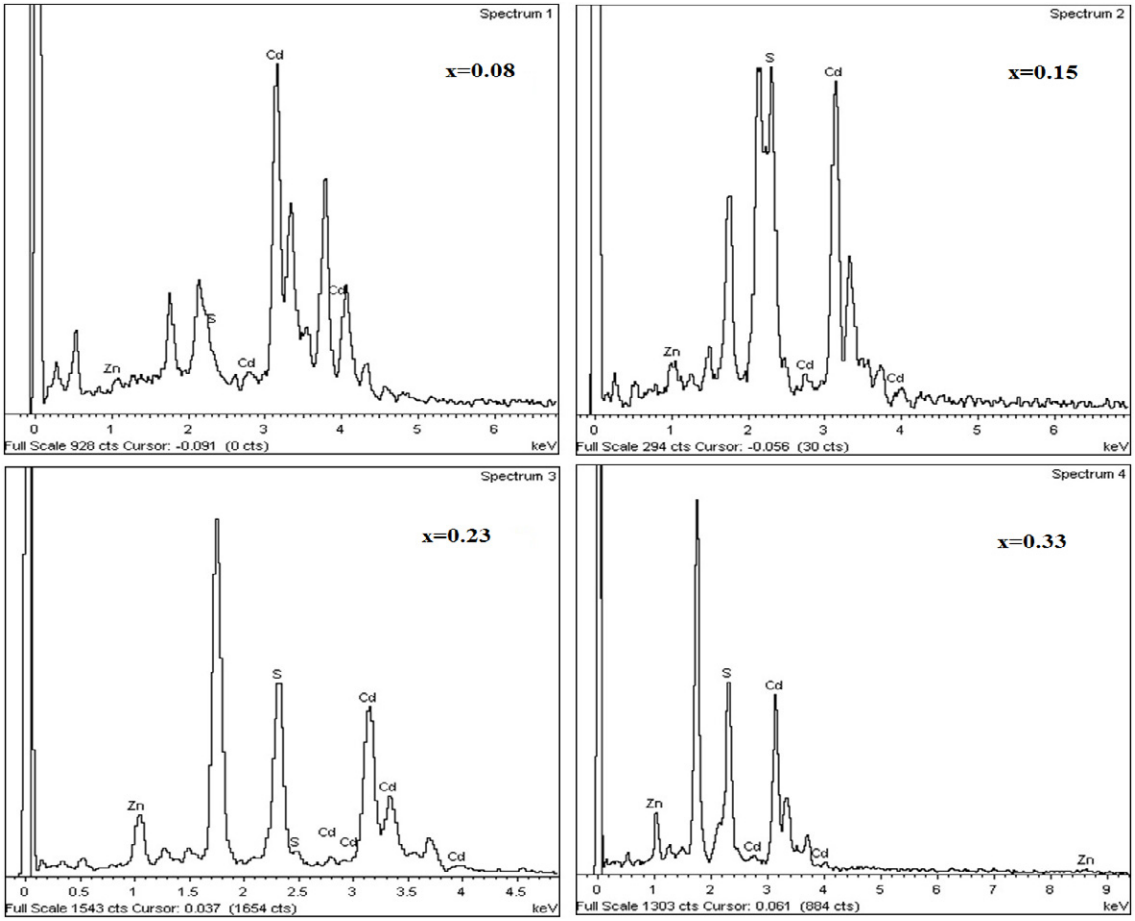

Fig. 1. EDX patterns of $Zn_xCd_{1-x}S$ for low value of 'x'

Table 2. Elemental compositions and value of 'x' of $Zn_xCd_{1-x}S$ thin films from EDX analysis with RF power variation of CdS, ZnS

RF Power (Watt)		Elemental composition of $Zn_xCd_{1-x}S$ from EDX						Composition 'x' from EDX result
CdS	ZnS	Atomic (%)			Weight (%)			
		Zn	Cd	S	Zn	Cd	S	
40	5	7.45	85.74	6.81	6.95	90.98	2.07	0.08
40	7	7.88	44.7	47.42	7.45	71.40	21.15	0.15
40	8	14.90	39.72	45.38	11.79	62.42	25.79	0.23
40	11	18.02	36.60	45.38	16.37	62.49	21.14	0.33

Strong peaks of cadmium (Cd) and sulphur (S) were observed in the EDX spectrum as the concentrations of these elements were high compared to that of zinc (Zn). The other peaks of the spectrum indicated the presence of oxygen, silicon etc. which appeared due to the bare glass substrate. The RF power variation of CdS and ZnS targets for attaining desired composition of the films and

percentage concentration of the elements in the films are given in Table 2. The minimum RF power of ZnS was 5 W because RF power of ZnS less than 5 W could not be possible for our co-sputtering as plasma went out for that RF power and no deposition was possible. The sample with Zn atomic concentration 14.90% (x=0.23) was selected for annealing treatment as $Zn_xCd_{1-x}S$ thin films attaining Zn<0.2 did not show significant bandgap in comparison to CdS.

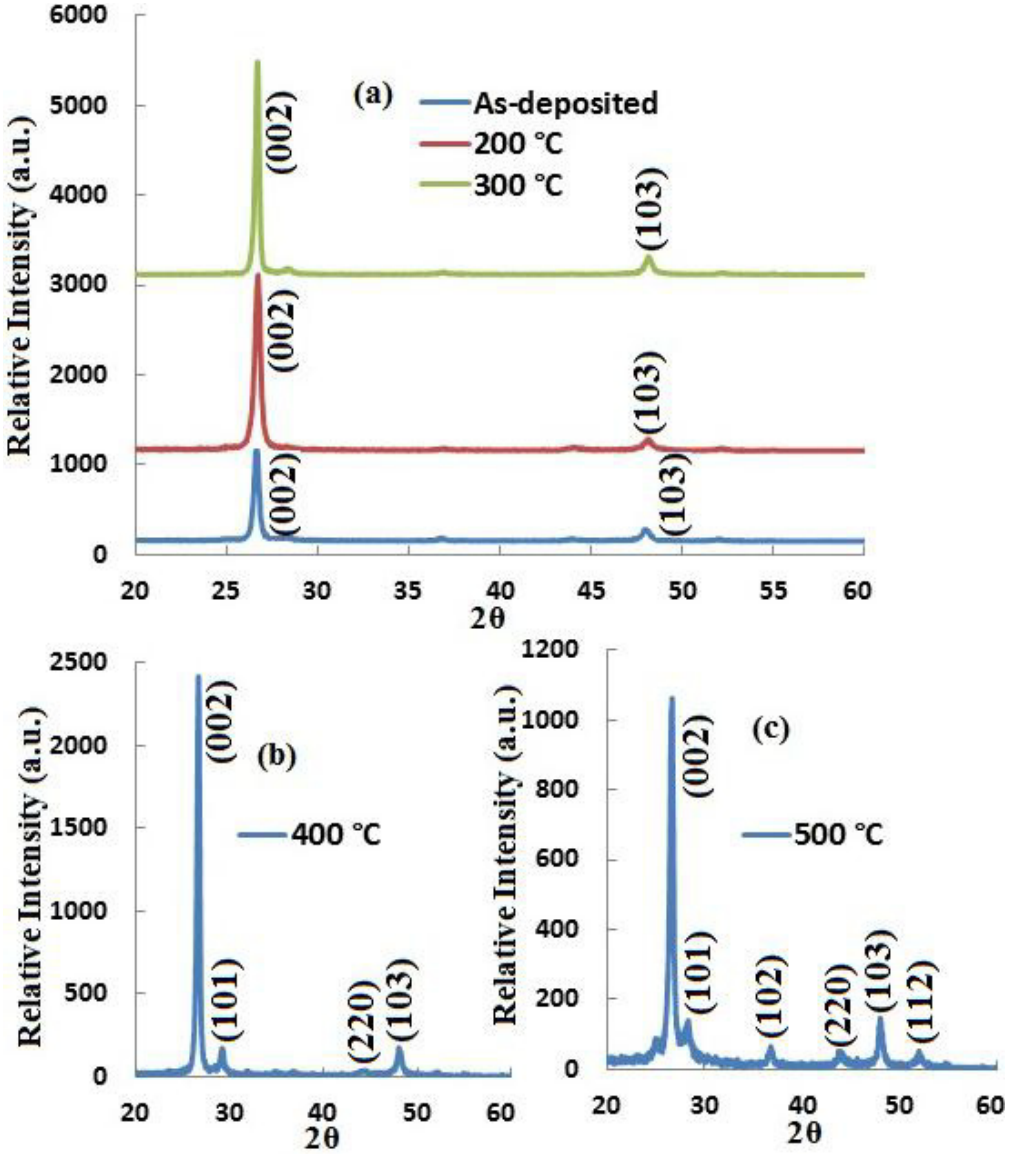

Fig. 2. XRD spectra of $Zn_{0.23}Cd_{0.77}S$ thin films (a) as-deposited, 200 ^{0}C, 300 ^{0}C (b) 400 ^{0}C (c) 500 ^{0}C

Figure 2 above shows XRD patterns of the as-deposited and annealed $Zn_{0.23}Cd_{0.77}S$ thin films. The as-deposited $Zn_{0.23}Cd_{0.77}S$ thin films show three diffraction peaks of (002), (102) and (103). The peak

intensities of (002) diffraction line increases with the increasing of annealing temperature up to 400 ºC. However, decreasing trend of peak intensity for (002) diffraction peak is observed for annealing temperature 500 ºC. For the films annealed at 400 ºC and 500 ºC some new peaks (101), (220) and (112) begin to appear. Additional thermal energy gained from the annealing phenomenon enhances the crystallisation process. In these entire duration of annealing temperature variation, the (002) diffraction peak is present, indicating that the thin film has a hexagonal structure. All of the peaks are identified as diffraction peaks matching to JCPDS cards no. 80-0006, 40-0834, 40-0835, 24-1136, 41-1049, 36-1450 and 49-1302. Higher annealing temperature yields better crystallinity of $Zn_{0.23}Cd_{0.77}S$ thin films which is reflected in the XRD results.

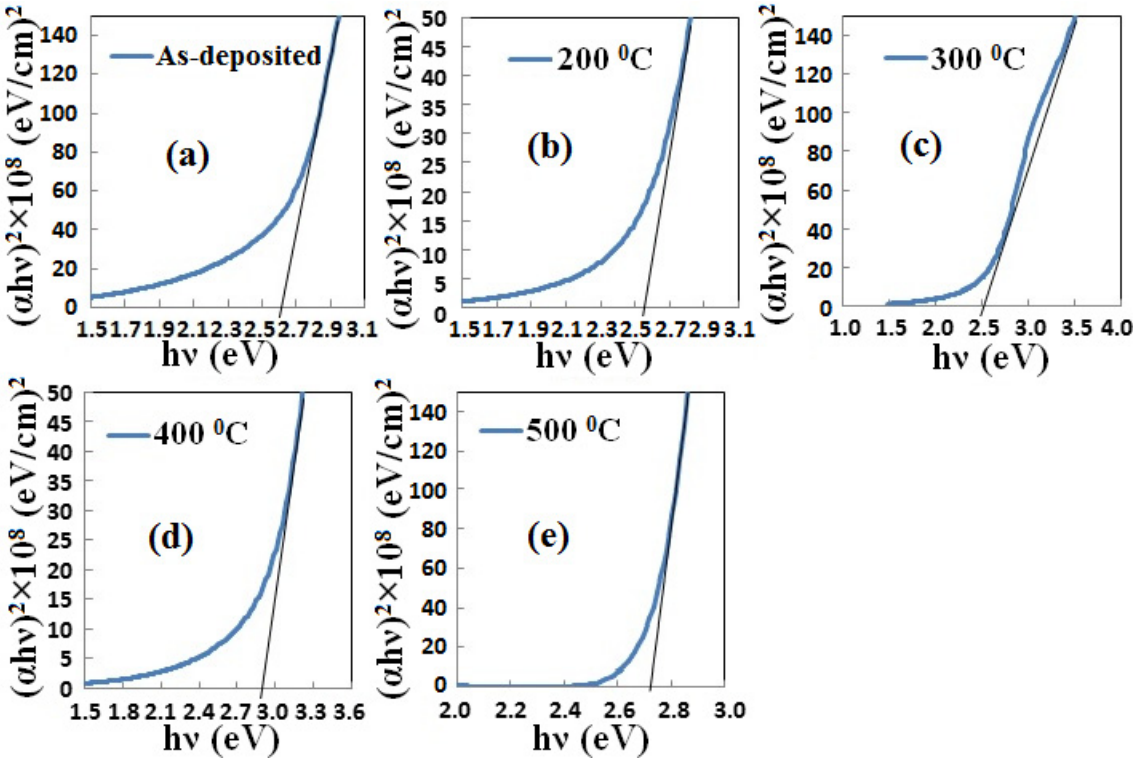

Fig. 3. $(\alpha h\nu)^2$ plotted against hν to determine the bandgap of $Zn_{0.23}Cd_{0.77}S$ thin films for (a) as-deposited and annealing temperature (b) 200 ºC (c) 300 ºC (d) 400 ºC (e) 500 ºC

Figure 3 shows the experimentally observed values of $(\alpha h\nu)^2$ plotted against hν for as-deposited and annealing temperatures to obtain the energy bandgap from the absorption spectra. From the model for direct allowed transitions, the value of the energy bandgap is given by the intercept of the straight line with the hν axis. The energy bandgaps of the films varied with the variation of annealing temperatures. With increasing annealing temperature up to 300 ºC, the energy bandgap of the films significantly decreases while increasing in annealing temperature at 400 ºC can cause abruptly increase in the bandgap and again follows decreasing trend for 500 ºC but the bandgap is more than that of 300 ºC and lower. The annealing can cause increase in the grain size which decrease the apparent bandgap. The decrease in the bandgap by low temperature annealing (<400 ˚C) may have been due to possible increase in the crystalline nature of the material [18]. The increase in bandgap by annealing at 400 ºC may have been due

to the appearing new peaks in the XRD patterns [19]. The bandgap follows decreasing trend for 500 ºC than 400 ºC. However, the bandgap at 500 ºC is more than that of 300 ºC and lower annealing temperatures. The extrapolated bandgap values for $Zn_{0.23}Cd_{0.77}S$ thin films at as-deposited and annealing temperatures at 200 ºC, 300 ºC, 400 ºC and 500 ºC are estimated around 2.62 eV, 2.55 eV, 2.5 eV, 2.9 eV and 2.72 eV, respectively. Melo *et al.* [20] reported the similar behavior of bandgap of CBD-CdS. However, the bandgap begins to increase at 300 ^{0}C in the reported works [21], and the increase is much more gradual.

The optical transmission spectra of $Zn_{0.23}Cd_{0.77}S$ thin films are shown in Fig. 4 annealed at different temperatures. The spectral transmittance begins to fall in longer wavelength regions for films annealed at lower temperatures while annealing temperature beyond 400 ºC provided the shift of absorption edge to the shorter wavelength regions. The average transmission is higher for high annealing temperature and highest for annealing temperature of 400 ºC.

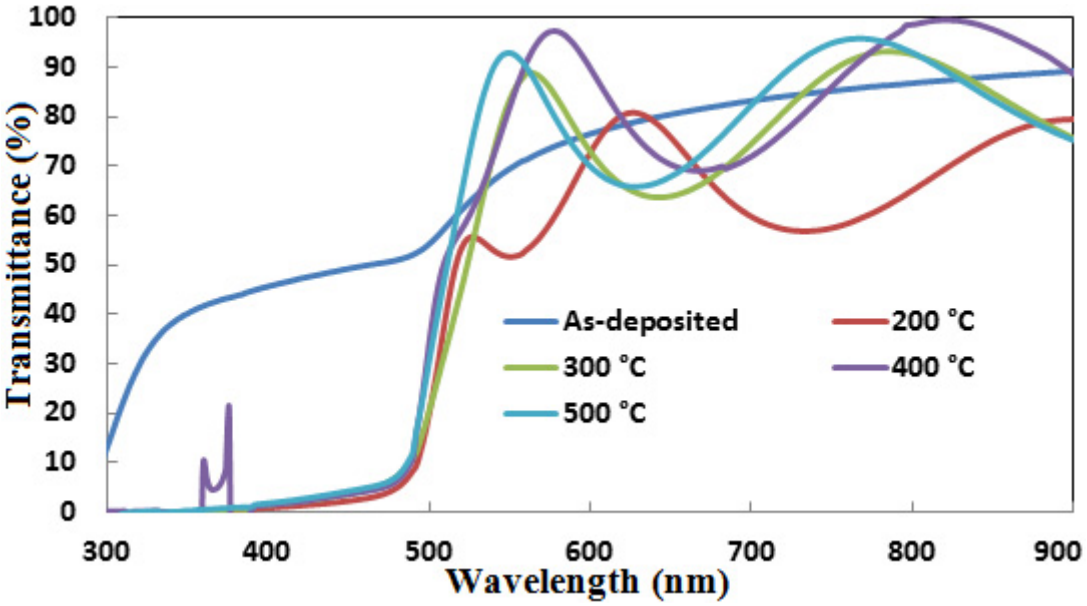

Fig. 4. Transmission spectra of $Zn_{0.23}Cd_{0.77}S$ films annealed at different annealing temperatures

In this study, FESEM images were taken for 50 KX magnifications to allow a review of the detail growth mechanism of the annealed $Zn_{0.23}Cd_{0.77}S$thin films. Figure 5 below shows FESEM surface images of $Zn_{0.23}Cd_{0.77}S$ thin films for as-deposited and different annealing temperatures. In the films annealed at low temperature, clusters of grains with various sizes were present whereas big sized cluster of grains were developed in the films annealed at 200 ºC and 300 ºC. The cluster of grains are converted to isolated grains in the films annealed at 400 ºC and 500 ºC in which grain size is larger for 400 ºC annealed films than that of 500 ºC. However, more compaction is observed between the grains of annealed films at 500 ºC than that of 400 ºC and it seems that the clusters of grains have just begun to convert to isolated grains for the films annealed at 400 ºC.

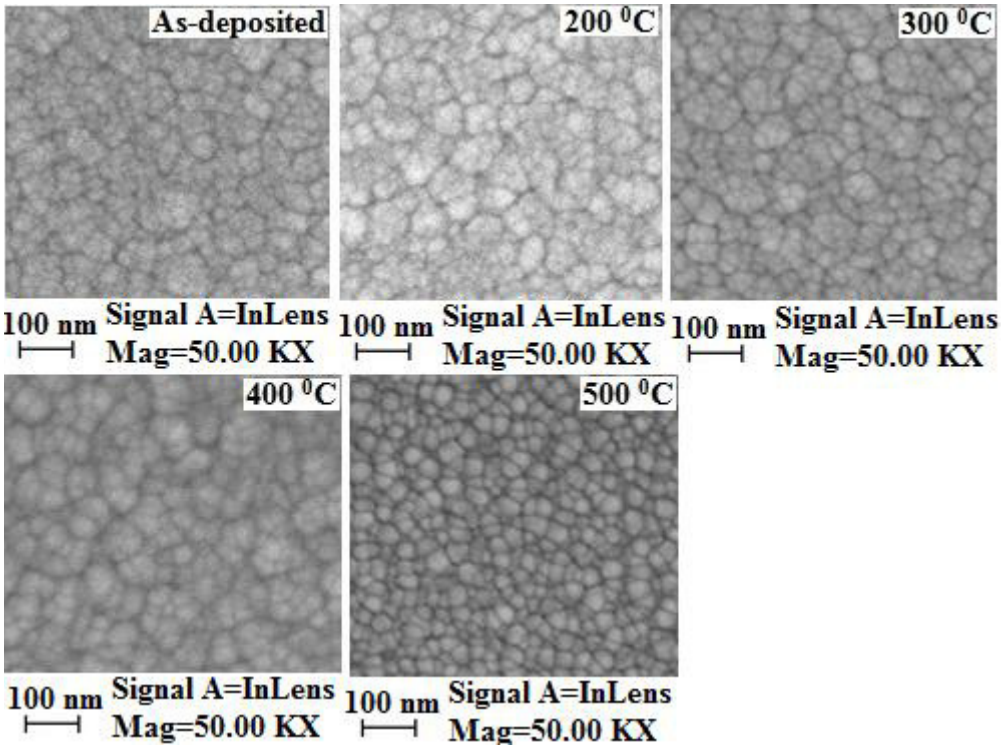

Fig. 5. SEM images of $Zn_{0.23}Cd_{0.77}S$ for as-deposited and different annealing temperatures

4. Conclusions

The $Zn_xCd_{1-x}S$ thin films for low Zn concentration were successfully deposited on glass substrates by co-sputtering of CdS and ZnS solid targets. This is the first time report of the influence of annealing treatment on $Zn_xCd_{1-x}S$ thin films prepared by co-sputtering of CdS and ZnS. After carrying out various optimisations, the results of characterized samples and the film properties have been analysed. Investigations show that higher annealing temperatures result in films of better crystallinity, higher optical transmission, larger isolated grains. However, isolated grains, bandgap and average transmittance of the films are the highest for annealing temperature of 400 ºC. This feature indicates that the $Zn_xCd_{1-x}S$ film properties for low Zn content at annealing temperature 400 ºC are suitable for solar photovoltaic applications, especially as a window layer for CdTe solar cells by tuning the bandgap to suitable values upon annealing, which is 2.9 eV at achieved at the annealing temperature of 400 ºC in this study.

Acknowledgement

This work is supported by the department of Electrical, Electronic and Systems Engineering and Solar Energy Research Institute (SERI), Univeresiti Kebangsaan Malaysia (UKM), Malaysia, through the research grant Zamalah UKM 2011 and the Ministry of Education grant with code ERGS/1/2012/TK07/UKM/01/4.

References

[1] Oladeji IO, Chow L, Ferekides CS, Viswanathan V, Zhao Z.Metal/CdTe/CdS/$Cd_{1-x}Zn_xS$/TCO/glass: a new CdTe thin film solar cell structure. *Solar Energy Materials Solar Cells* 2000;**61**:203-11.

[2] Matin MA, Aliyu MM, Quadery AH, Amin N. Prospects of novel front and back contacts for high efficiency cadmium telluride thin film solar cells from numerical analysis. *Solar Energy Materials Solar Cells* 2010;**94**:1496-1500.

[3] Amin N, Sopian K, Konagai M. Numerical modeling of CdS/CdTe and CdS/CdTe/ZnTe solar cells as a function of CdTe thickness. *Solar Energy Materials Solar Cells* 2007;**91**:1202-8.

[4] Chelvanathan P, Hossain M I , Amin N. Performance analysis of copper–indium–gallium–diselenide (CIGS) solar cells with various buffer layers by SCAPS. *Current Applied Physics* 2010; **10**: S387-S391.

[5] Chavhan S, Sharma RP. Growth, structural and optical transport properties of nanocrystal $Zn_xCd_{1-x}S$ thin films deposited by solution growth technique for photosensorapplications. *Journal of Physical Chemistry and Solids*2005;**66**:1721-6.

[6] Ferekides C, Britt J, Ma Y, Killian L. High efficiency CdTe solar cells by close spaced sublimation. *Proc. 23rd IEEE Photovoltaic Specialists Conf.*, Louisville, KY, 1993, pp. 389-393.

[7] Chu TL. Thin film cadmium telluride solar cells, final technical progress report. *SERl sub-contract XL-3-03122-1*, Dallas, Texas, 1985.

[8] DevancyWE, Chen WS, Stewart JM, Mickelsen RA. Structure and properties of high efficiency ZnO/CdZnS/$CuInGaSe_2$ solar cells. *IEEE Trans. Electron Devices* 1990;**37**:428-33

[9] Ray SC, Karanjai MK, DasGupta D. Deposition and characterization of $Zn_xCd_{1-x}S$ thin films by the dip technique. *Thin Solid Films* 1998;**322**:117-22.

[10] Menner R, Dimmler B, Mauch RH, Schock HW. II-VI compound thin film for windows in heterojunction solar cells. *J. Cryst Growth* 1988;**86**:906-11.

[11] Yamaguchi T,Yamamoto Y, Tanaka T, DemizuY, Yoshida A. (Cd,Zn)S thin films prepared by chemical bath deposition for photovoltaic devices. *Thin Solid Films* 1996; **281-282**: 375-8.

[12] Hossain MS, Amin N, Razykov T. Prospects of back contacts with back surface fields in high efficiency $Zn_xCd_{1-x}S$/CdTe solar cell from numerical. *Chalcogenide Letters* 2011;**8**: 187-98.

[13] RazykovTM.Physical properties of II–VI binary and multi-component compound films and heterostructures fabricated by chemical vapour deposition.*Thin Solid Films*1988; **164**: 301-08.

[14] Tian C, Tang R, Hu S, Li W, Feng L, Zhang J,Wu L. Comparative studies of CdZnS thin films at low zinc content prepared by vacuum evaporation and CBD. *Adv. Mat. Research* 2011; **225-226**:784-8.

[15] Raviprakash Y, BangeraKasturi V,Shivakumar GK. Growth, structural and optical properties of $Cd_xZn_{1-x}S$ thin films deposited using spray pyrolysis technique. *Current Applied Physics* 2010;**10**: 193-8.

[16] Sanap VB,Pawar PH. Study of chemical bath deposited nanocrystalline CdZnS thin films. *J. Opt. Biomed. Mat.* 2011; **3**:39-43.

[17] Mesic B, Schroeder H. Properties of TaSiN thin films deposited by reactive radio frequency magnetron sputtering. *Thin Solid Films* 2012;**520**:4497-4500.

[18] Chavhan S. Sharma RP. Growth, structural and optical transport properties of nanocrystal $Zn_{1-x}Cd_xS$ thin films deposited by solution growth technique (SGT) for photosensorapplications. *J.Phy. Chem. Solid* 2005; **66**: 1721-6.

[19] Bouroushian M, Loizos Z, Spyrellis N, Maurin G. Hexagonal cadmium chalcogenide thin films prepared by electrodeposition from near-boiling aqueous solutions. *Appl. Surf. Sci.* 1997;**115**: 103-110.

[20] de Melo O, Hernández L, Zelaya Angel O, Lozada Morales R, Becerril M, Vasco E. Low resistivity cubic phase CdS films by chemical bath deposition technique. *Appl. Phys. Lett.* 1994;**65**:1278-80.

[21] Gaewdang Ng,Gaewdang T. Investigations on chemically deposited $Cd_{1-x}Zn_xS$ thin films with low Zn content. *Matt. Letters* 2005; **59**:3577-84.